

PHOTOPROTONS FROM Pr^{141}

V. G. SHEVCHENKO and B. A. YUR'EV

Institute of Nuclear Physics, Moscow State University

Submitted to JETP editor June 6, 1961

J. Exptl. Theoret. Phys. (U.S.S.R.) 41, 1421-1426 (November, 1961)

The angular and energy distributions and the yields of photoprotons from Pr^{141} are measured for maximum bremsstrahlung energies of 22.5 and 33.5 Mev. The results indicate that the maximum photoprotion production cross section corresponds to γ quanta above 22 Mev and that the absorption of γ quanta in this energy region is chiefly of quadrupole character.

PROTON emission resulting from the dipole absorption of γ radiation is strongly inhibited by the high Coulomb barrier of heavy nuclei, so that the photodisintegration of these nuclei results mainly in neutron emission. It thus becomes possible to distinguish protons resulting from the quadrupole absorption of γ radiation. The cross section for the latter process must lie in a higher energy range, so that some of the emitted protons will have high energies.^[1]

Several investigations of angular and energy distributions of photoprotons from heavy nuclei have been published.^[2-5] In almost all instances bremsstrahlung having $E_{\gamma\text{max}} = 22-24$ Mev was used, whereas quadrupole resonance absorption evidently occurs at somewhat higher energy. Exceptions occurred in the photodisintegration of Pb and Bi for $E_{\gamma\text{max}} = 24$ Mev,^[2,3] where strong asymmetry was observed favoring small angles. This effect apparently results from the fact that for heavy nuclei such as Pb and Bi, even at the given relatively low energies the total γ -ray absorption cross section involves a considerable contribution from quadrupole transitions.

In the present work bremsstrahlung having $E_{\gamma\text{max}} = 22.5$ and 33.5 Mev was used to investigate the energy and angular distributions of protons from the photodisintegration of Pr^{141} .

EXPERIMENTAL PROCEDURE

Our bremsstrahlung source was the 35-Mev betatron of the Institute of Nuclear Physics at Moscow State University. The experimental arrangement is shown in Fig. 1. The γ -ray beam passed through a lead collimator 32 cm thick and a clearing magnet before impinging on the target in the vacuum chamber. The target was metallic praseodymium foil 31.1 mg/cm² thick placed at an

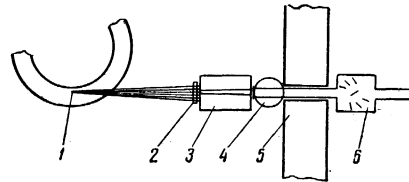


FIG. 1. Arrangement of apparatus: 1 — betatron target, 2 — thin-walled monitor chamber, 3 — collimator, 4 — clearing magnet, 5 — shielding wall, 6 — vacuum chamber in magnetic field.

angle of 30° to the γ -ray beam. The principal impurities in the target were not more than 1.5% of rare earth elements and not more than 0.1% of other elements.

Protons leaving the target were registered on photoplates with type T-3 NIKFI emulsion 400 μ thick disposed in the chamber at angles of 30, 45, 60, 75, 90, 120, 135, and 150° with respect to the γ -ray beam. Type T-3 plates were used to permit an increased radiation dose, since this emulsion is considerably less sensitive to the electron background than the type Ya-2 emulsion ordinarily used. In order to reduce the electron background of plates placed at acute angles, during irradiation

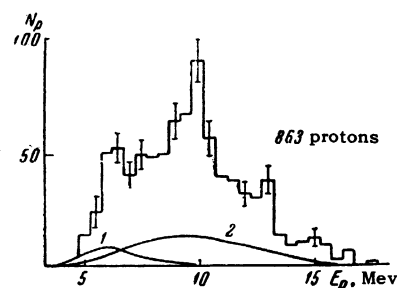


FIG. 2. Energy distribution of photoprottons from Pr^{141} produced by radiation having $E_{\gamma\text{max}} = 22.5$ Mev. The continuous curve 1 is the computed spectrum of evaporation protons; curve 2 is the computed spectrum of direct-photo-effect protons.

Table I. Parameters of type (1) curves approximating the angular distributions of photoprottons from Pr^{141} , and values of $\sigma_{E_2}/\sigma_{E_1+E_2}$ derived from the $\sigma_{E_2}/\sigma_{E_1} = p^2/5$

$E_{\gamma\text{max}}, \text{Mev}$	Proton energy, Mev	a	b	p	$\sigma_{E_2}/\sigma_{E_1+E_2}, \%$
22.5	4.5–7.25	31	15.7	0.42	~3
	7.25–11.25	44	66	0.32	~2
	≥ 11.25	12	27.5	0.44	~4
33.5	4.5–7.25	71	23.4	1.4	~30
	7.25–11.25	153	57	2.2	~50
	≥ 11.25	50	71.4	1.8	~40

the vacuum chamber was placed in a ~ 600 -oe magnetic field that deflected electrons emitted from the target to prevent their direct impingement on the emulsion. The permissible radiation dose thus became several times larger.

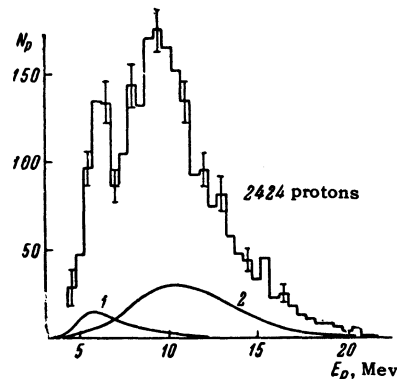


FIG. 3. Energy distribution of photoprottons from Pr^{141} produced by radiation having $E_{\gamma\text{max}} = 33.5$ Mev. The notation is the same as in Fig. 2.

The position of the beam axis relative to the center of the chamber was determined by means of x-ray film and was monitored by comparing the effects on two plates positioned at 90° angles symmetrically with respect to the target center.

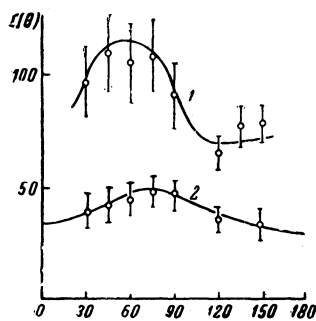


FIG. 4. Angular distribution of 4.5–7.25 Mev photoprottons (first group): 1 – for $E_{\gamma\text{max}} = 33.5$ Mev; 2 – for $E_{\gamma\text{max}} = 22.5$ Mev. The continuous approximating curves have the parameters given in Table I.

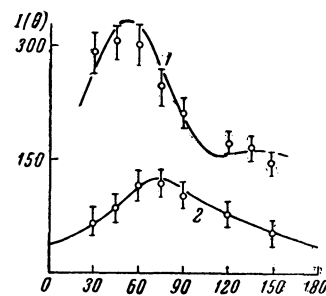


FIG. 5. Angular distribution of 7.25–11.25 Mev photoprottons (second group): 1 – for $E_{\gamma\text{max}} = 33.5$ Mev; 2 – for $E_{\gamma\text{max}} = 22.5$ Mev.

Absolute solid angles were determined graphically and by calculation. In scanning we selected tracks that started at the emulsion surface, corresponding to protons having energies ≥ 1.0 Mev and originating in the irradiated portion of the target. Proton energy was determined from the range-energy curve for Ilford C-2 emulsion, with a correction for the $\sim 5\%$ density difference between T-3 and C-2 emulsions. A correction was also introduced for energy loss in the target.

EXPERIMENTAL RESULTS

Figures 2 and 3 show the energy distributions of protons produced in the photodisintegration of

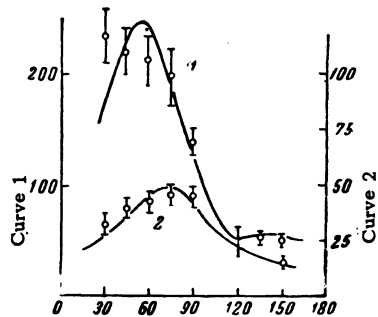


FIG. 6. Angular distribution of photoprottons ≥ 11.25 Mev (third group): 1 – for $E_{\gamma\text{max}} = 33.5$ Mev; 2 – for $E_{\gamma\text{max}} = 22.5$ Mev.

Table II. Principal E1 and E2 proton transitions
of Pr¹⁴¹

Multipolarity	Transition	No. of nucleons in initial state	Proton energy, Mev*	γ -transition energy, Mev
E1	$2d_{5/2} \rightarrow 2f_{7/2}$	1	5—7	11—13
	$2d_{5/2} \rightarrow 2f_{5/2}$	1	8—10	13—15
	$1g_{7/2} \rightarrow 1h_{9/2}$	8	7—9	14—16
	$1g_{7/2} \rightarrow 2f_{7/2}$	8	5—7	12—14
	$1g_{7/2} \rightarrow 2f_{5/2}$	8	8—10	15—17
	$1g_{7/2} \rightarrow 2f_{3/2}$	10	5—7	17—19
	$2p_{1/2} \rightarrow 3d_{5/2}$	2	14—16	26—28
	$2p_{3/2} \rightarrow 3d_{5/2}$	4	13—15	26—28
E2	$1g_{9/2} \rightarrow 1i_{13/2}$	10	4—6	16—18
	$1g_{9/2} \rightarrow 1i_{11/2}$	8	12—14	19—21
	$2d_{5/2} \rightarrow 2g_{9/2}$	1	10—12	16—18
	$2d_{5/2} \rightarrow 2g_{7/2}$	1	13—15	19—21
	$2d_{5/2} \rightarrow 4s_{1/2}$	1	14—16	20—22
	$2p_{1/2} \rightarrow 2f_{5/2}$	2	4—6	16—18
	$2p_{1/2} \rightarrow 2f_{3/2}$	4	2—4	15—17
	$2p_{3/2} \rightarrow 2f_{5/2}$	4	4—6	17—19
	$1f_{5/2} \rightarrow 1h_{9/2}$	6	4—6	20—22
	$1f_{7/2} \rightarrow 1h_{9/2}$	8	4—6	22—24

*Proton and γ -ray energies in the case of E1 absorption have been increased by 4—5 Mev compared with single-particle calculations [5] in order to take account of residual interactions. This has not been done for E2 transitions, since the magnitudes of the residual interactions are unknown for highly excited states.

Pr¹⁴¹ by γ radiation with $E_{\gamma\text{max}} = 22.5$ and 33.5 Mev. The graphs have taken into account the background, which was $\sim 5\%$ on the average, except at 30° , where the background was $\sim 20\%$. The spectra included a small contribution from deuterons, tritons, and α particles, whose tracks were not identified. This contribution evidently did not exceed a few percent.

The energy spectra exhibit overall similarity. Both spectra have peaks at ~ 6 and ~ 10 Mev, which are more prominent in the case of $E_{\gamma\text{max}} = 33.5$ Mev. The declining portions of the two spectra have approximately identical shapes.

Figures 4—6 show the angular distributions of different photoproton groups corresponding to the aforementioned peaks at 6 and 10 Mev and the declining portion of the spectrum.

The experimental values were fitted approximately by curves of the form

$$a + b \sin^2 \theta (1 + p \cos \theta)^2. \quad (1)$$

The parameters of the approximating curves are given in Table I. The figures and the table show that the angular distributions of photoparticles for $E_{\gamma\text{max}} = 33.5$ Mev have peaks at smaller angles than for $E_{\gamma\text{max}} = 22.5$ Mev. The estimated yields

are $\sim 8 \times 10^4$ and $\sim 1.3 \times 10^5$ protons/mole-roentgen for $E_{\gamma\text{max}} = 22.5$ and 33.5 Mev, respectively. The yield increases markedly with $E_{\gamma\text{max}}$.

DISCUSSION OF RESULTS

A comparison of the photoparticle yields from Pr¹⁴¹ for $E_{\gamma\text{max}} = 22.5$ and 33.5 Mev shows that over 50% of the total proton yield for $E_{\gamma\text{max}} = 33.5$ Mev (including $\sim 40\%$ of the first proton group, $\sim 55\%$ of the second group, and $\sim 70\%$ of the third group) is produced by γ radiation having $E_{\gamma\text{max}} > 22.5$ Mev. This indicates that the maximum photoproduction cross section in Pr¹⁴¹ corresponds to γ radiation having energy > 22.5 Mev. A comparison of the experimental yields with calculations based on the evaporation model [4] and the direct photoeffect [4,6] shows that neither model can account for the results. The estimated photoparticle yield based on the statistical model for Pr¹⁴¹ was smaller by a factor of 15 to 20 than the experimental value. The proton contribution from the direct photoeffect is somewhat larger, although [6] shows that our observed total yield is 4 to 5 times greater. As could be expected, a large fraction of the observed photoparticles result from direct resonance absorption of γ radiation.

Good agreement with experiment has recently been obtained in [7] by calculating the total γ -radiation absorption cross section on the shell model with mixed configurations. However, such calculations are possible practically only for doubly magic nuclei. Since this did not apply in our case, we calculated the energies of dipole proton transitions using single-particle levels computed for intermediate and heavy nuclei. [8]

These calculations did not take into account the residual interactions between nucleons, which we evaluated as follows. Since data are lacking for the $\text{Pr}^{141}(\gamma, p)$ cross section all comparisons between calculations and experiment were performed for the (γ, n) reaction. The center of dipole neutron transitions in the single-particle shell model was compared with the maximum $\text{Pr}^{141}(\gamma, n)$ cross section obtained experimentally. [9, 10] The difference observed here gave 4–5 Mev for the residual interactions. Practically identical magnitudes were assumed for the residual interaction in Pr^{141} in the cases of both proton and neutron transitions, and the center of dipole proton transitions was found with this residual interaction taken into account. Table II gives the results for individual transitions. The center of dipole proton transitions is seen to correspond to 16–17 Mev γ rays and the maximum cross section, for γ rays having energy > 22.5 Mev, cannot be accounted for by direct resonance dipole transitions.

This is confirmed by the additional interesting result that very different angular distributions of photoprotons are obtained for $E_{\gamma\max} = 22.5$ and 33.5 Mev. The character of γ -ray absorption changes considerably when E_{γ} increases above 22 Mev. Considerable asymmetry is observed with respect to 90° and the angular distribution peak is shifted toward smaller angles. For $E_{\gamma} < 22$ Mev, on the other hand, the proton angular distribution is practically symmetrical with respect to 90°.

The approximation of angular distributions by curves plotted from Eq. (1) furnishes only a rough estimate of the quadrupole absorption contribution, which according to Table I would reach 50%. However, the results are in good agreement with the fact that the quadrupole transition center is in the region $E_{\gamma} > 22$ Mev, as can be seen by analyzing the E2 transition energies in Table II.

The energy spectra exhibit two peaks, for 6–7 and 9–10 Mev protons, respectively. For $E_{\gamma\max} = 22.5$ Mev these peaks are poorly resolved, while for $E_{\gamma\max} = 33.5$ Mev they are clearly defined at the same energies. It appears from Table I that

the principal peak of the spectrum for $E_{\gamma\max} = 22.5$ Mev corresponds to the transitions $1g_{7/2} \rightarrow 1h_{9/2}$ and $1g_{7/2} \rightarrow 2f_{5/2}$, producing 8–10 Mev protons. The peak at 6–7 Mev can be associated with $1g_{9/2} \rightarrow 2f_{7/2}$ and $2d_{5/2} \rightarrow 2f_{7/2}$ transitions. In the spectrum for $E_{\gamma\max} = 33.5$ Mev these peaks are more pronounced, as already mentioned, and correspond to the enumerated dipole transitions as well as quadrupole transitions. The most intense of the latter, $1g_{7/2} \rightarrow 1i_{11/2}$ and $2d_{5/2} \rightarrow 2g_{9/2}$, produce 10–14 Mev protons, whereas 5–6 Mev protons result from $1g_{9/2} \rightarrow 1i_{13/2}$ and $1f_{5/2} \rightarrow 1h_{9/2}$ transitions and some others. It is not clear why the peaks for $E_{\gamma\max} = 33.5$ Mev are more pronounced. The analysis of the energy spectra is greatly hampered generally by the impossibility, in our case, of taking into account the effects resulting from the mixing of configurations.

Our results lead to the conclusion that the maximum photoprotton production cross section of Pr^{141} corresponds to γ radiation in the energy region above 22 Mev, and that γ -ray absorption in this region is mainly of quadrupole character.

In conclusion the authors wish to thank V. V. Balashov and V. G. Neudachin for discussions of the results, S. Ovchinnikov for assistance in treating the results, and the betatron crew.

¹ Neudachin, Shevchenko, and Yudin, II Vsesoyuznaya konferentsiya po yadernym reaktsiyam pri malykh i srednikh energiyakh (Report at 2nd All-Union Conference on Nuclear Reactions at Low and Intermediate Energies), Moscow, 1960.

² M. E. Toms and W. E. Stephens, Phys. Rev. **92**, 362 (1953).

³ M. E. Toms and W. E. Stephens, Phys. Rev. **98**, 626 (1955).

⁴ W. K. Dawson, Can. J. Phys. **34**, 1480 (1956).

⁵ E. D. Makhnovskii, JETP **38**, 95 (1960), Soviet Phys. JETP **11**, 70 (1960).

⁶ E. D. Courant, Phys. Rev. **82**, 703 (1951).

⁷ Balashov, Shevchenko, and Yudin, Nuclear Phys. **27**, 323 (1961).

⁸ A. Schröder, Nuovo cimento **7**, 461 (1958).

⁹ L. Katz and J. Chidley, in: Yadernye reaktsii pri malykh i srednikh energiyakh (Nuclear Reactions at Low and Intermediate Energies), Moscow, 1958, p. 371.

¹⁰ J. H. Carver and W. Turchinetz, Proc. Phys. Soc. (London) **73**, 110 (1959).